



Experimental investigation of mid-spatial frequency surface textures on fused silica after computer numerical control bonnet polishing

Wei-Ren Huang¹ · Tsung-Yueh Tsai¹ · Yi-Jyun Lin² · Ching-Hsiang Kuo³ · Zong-Ru Yu³ · Cheng-Fang Ho³ · Wei-Yao Hsu⁴ · Hong-Tsu Young¹

Received: 5 November 2019 / Accepted: 29 April 2020 / Published online: 26 May 2020
© Springer-Verlag London Ltd., part of Springer Nature 2020

Abstract

Automated bonnet polishing is achieved using computer numerical control (CNC) technology. However, owing to specific toolpaths, CNC bonnet polishing is generally accompanied by the mid-spatial frequency (MSF) of surface textures on polished surfaces that could produce surface ripples or waviness and degrade image quality. In this study, the MSF surface textures on fused silica are investigated by developing a CNC bonnet polishing technique using a cerium oxide-filled polyurethane pad (LP66)—a cellular polyurethane material designed to handle high flatness and surface finishing requirements for optical glass materials. To minimize the MSF, optimal combinations of various polishing parameters, including tool offset, head speed, track spacing, and surface feed rate, are studied. Experimental results demonstrate that the head speed and feed rate significantly affect the surface texture during bonnet polishing. Although the tool offset does not cause surface textures, the material removal rate is affected. A series of optimization experiments is conducted, consequently leading to the effective removal of irregular surface ripples and a reduction of MSF errors. By optimizing the polishing parameters, extremely accurate surface quality is achieved, along with a root mean square error of 1.6 nm. These results demonstrate the potential applications of LP66 in CNC bonnet polishing for highly accurate freeform optical components.

Keywords Computer numerical control · Bonnet polishing · Optical glass · Mid-spatial frequency · Fused silica

1 Introduction

Advancements in photoelectric technology have led to a rapid growth of extremely accurate optical devices owing to the increasing demands for consumer products in various industries such as aerospace [1], defense, security, medicine [2], and mobile telecommunications. Because such products generally include ultra-high-resolution optical components, the

manufacture and development of highly accurate freeform optical components are immediately required to satisfy the fast-growing demand [3, 4]. Conventional processes for polishing optical glass involve semi-automated and, in some instances, manual polishing, both of which are labor- and time-intensive. The requirements of highly accurate surface quality and freeform geometric complexity pose considerable challenges regarding the fabrication of such optical components [5]. However, computer numerical control (CNC) subaperture bonnet polishing [6] is a suitable technology for polishing geometrically complex optical components made of difficult-to-machine materials. Moreover, bonnet polishing improves the peak-to-valley (PV) and root mean square (RMS) values of freeform optical components [7]. A major challenge in bonnet polishing is the prevention of mid-spatial frequency (MSF) errors [8], which often deteriorate the performance of optical systems.

In their study on polishing freeform optical components, Wang et al. [9] present a novel multi-jet polishing process and develop a polishing tool that can potentially perform high-efficiency polishing on medium-to-large

✉ Wei-Ren Huang
d01522027@ntu.edu.tw

¹ Mechanical Engineering Department, National Taiwan University, Taipei 106, Taiwan

² Laser and Inspection R&D Division, Contrel Technology Co., Ltd., Tainan, Taiwan

³ Taiwan Instrument Research Institute, National Applied Research Laboratories, Hsinchu 300, Taiwan

⁴ Laser Business Group, Contrel Technology Co., Ltd., Tainan 744, Taiwan

surfaces. Additionally, Wang et al. [10] develop a semi-rigid bonnet tool that has the advantages of high efficiency and determinacy for removing material on optical components. Furthermore, Belkhir et al. [11] observe that high-quality optical surfaces can be obtained by controlling the polishing pressure and friction coefficient form against the contact surface. Guo et al. [12] use the R-test to develop a method for measuring and reducing the virtual pivot (VP) error and further investigate the influence of the VP error on surface profiles. Cao et al. [13] present an experimental investigation that attempts to provide a better scientific understanding of material removal and surface generation characteristics in bonnet polishing. Pan et al. [14] modify the tool influence function (TIF) of bonnet polishing based on the interfacial friction coefficient, aiming to improve the modeling accuracy of the TIF such that the modeled results are much closer to the experimental results, thereby demonstrating the effectiveness of the modification. Most researchers focus on high-efficiency material removal and high-quality optical surfaces to achieve better surface generation on optical components fabricated by bonnet polishing, whereas PV and RMS errors directly affect the polishing quality of an optical surface and also accompany low to medium—and even high—spatial frequency errors.

To reduce MSF errors and obtain an extremely high-quality optical surface, the key optimization parameters of the surface texture is theoretically and experimentally investigated via CNC subaperture bonnet polishing on fused silica. In CNC bonnet polishing, the key parameters are feed rate, head speed, track spacing, and tool offset [15]. To further consider the MSF errors accompanying CNC polishing due to the specific tool path, the power spectral density (PSD) index was utilized in the observation and analysis of the magnitude and frequency of MSF errors.

2 Experimental setup

Experiments were designed to improve the quality of optical lens surfaces by optimizing the key polishing parameters and developing a strategy using CNC subaperture bonnet precession polishing. In the experiments, a Zeeko IRP 1000 7-axis CNC polishing machine (Fig. 1) was used to obtain an extremely high-quality optical surface. The polishing head was configured for seven axes, and the interior was inflated with compressed air. The bonnet tool was fitted with a 40-mm-diameter polyurethane polishing pad (LP66) filled with cerium oxide and an inflated flexible bonnet. The LP66 polishing pad [13] is a cellular polyurethane material designed to handle high

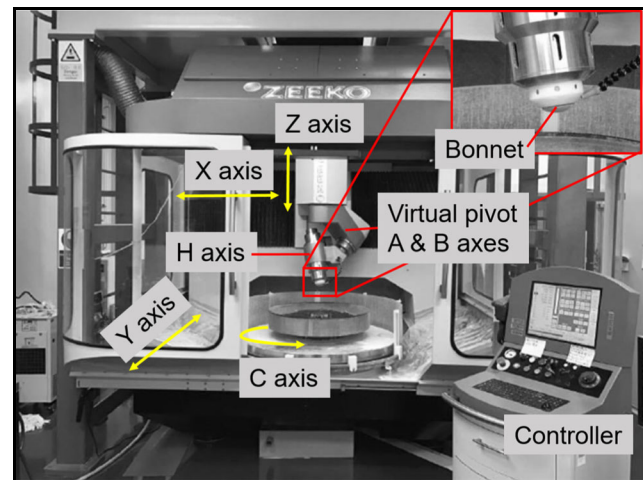


Fig. 1 ZEEKO IRP 1000 CNC polishing machine

flatness and surface finishing requirements for optical glass materials. The motion control method was CNC, as it satisfies several polishing requirements for large optical lenses [7], as shown in Fig. 2.

Fused silica glass (Nikon, NIFS Series) 40 mm in diameter was used as the workpiece, and the main constituent was SiO_2 . In addition to high head speed, slurry (comprising an aqueous suspension of cerium oxide abrasives and a specific gravity of 1.03) was used during bonnet polishing for cooling and lubricating the workpiece (Fig. 3) to obtain a high-quality optical lens surface. The LP66 polishing pad was attached to the bonnet (Fig. 4), thereby improving the surface quality of the fused silica glass. Finally, an aspheric stitching interferometer (QED-ASI interferometer) was used to observe and analyze the experimental results.

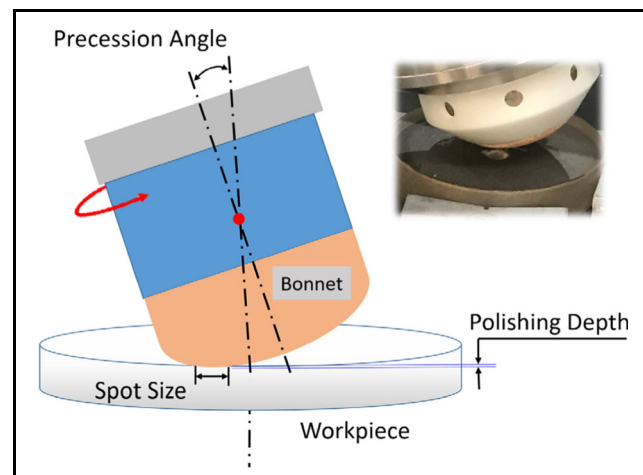


Fig. 2 Bonnet polishing method

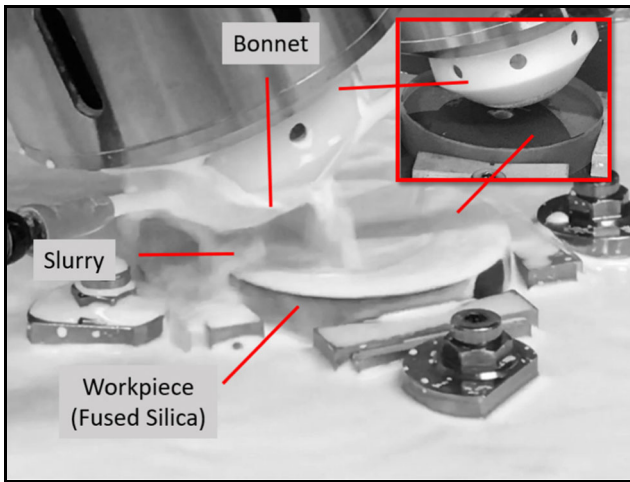


Fig. 3 Slurry used with ZEEKO IRP 1000

3 Analysis and discussion of experimental results

To examine the relationship of MSF errors with surface ripples, the effects of the tool offset, head speed, track spacing, and surface feed on the ripple error are analyzed. According to Preston [16], the material removal characteristics of bonnet polishing can be described by Eq. (1):

$$MRR = \kappa \times P \times V \tag{1}$$

where MRR denotes the material removal rate in mm³/s, κ is the Preston coefficient (constant), P is the contact pressure between the polishing bonnet and the workpiece in N/mm², and V is the velocity of the polishing bonnet relative to the workpiece in mm/s. This indicates that the bonnet polishing surface feed rate and track spacing are the key influencing factors of MSF error. If the surface feed rate is high, the con-



Fig. 4 Bonnet capped with LP66 polishing pad

tact time on the glass surface is short. Similarly, if the track spacing is large, there are few polishing paths.

3.1 Tool offset

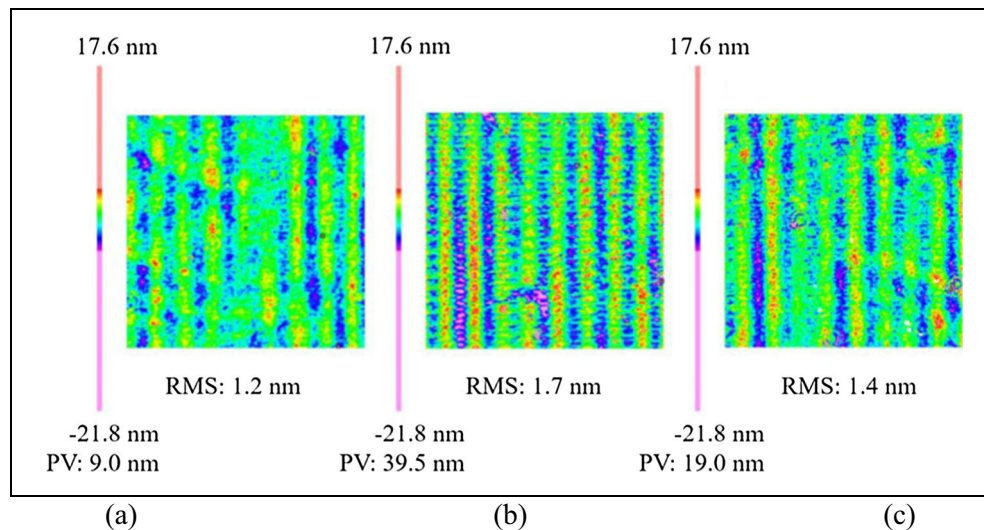
Theoretical and experimental studies on bonnet polishing [14] indicate that the mechanism of material removal is complex, and the tool offset is the dominant factor affecting the volumetric MRR. If the same dwell time is used, the same MRR can be achieved under identical polishing parameters. To further understand how the tool offset parameter affects the surface generation profile and MSF error, the experimental polishing parameters shown in Table 1 are applied.

In this experiment, three different tool offset parameters and the raster path are adopted. Other parameters such as the precession angle, head speed, track spacing, and surface feed are also considered. The adopted parameters of a general case are those recommended by Zeeko company, and focus is placed on the effect of the tool offset on the surface quality. To understand how different tool offsets affect the material removal depth and surface profile (including the PSD index), corresponding measurements obtained before and after the experiment are compared. The polishing bonnet pad became considerably worn with increased polishing depth. In the ideal machining range, the fused silica glass demonstrates no special wear patterns other than the normal ones shown in Fig. 5, indicating that the tool offset does not directly affect surface profile generation. The patterns parallel to the y-axis show regular spacing of approximately 3.3 mm. In contrast, the patterns parallel to the x-axis appear tight and unevenly spaced. The surface profiles are examined separately in both the x- and y-axis via the Fourier transform. The x-direction PSD curves in Fig. 6a reveal that the sample polished using the 0.25-mm tool offset shows a higher total PSD than the samples polished using the 0.2-mm and 0.3-mm tool offsets, indicating that the former sample exhibits significant surface rippling and that an increased PV easily dominates the surface profile. Overall, the samples polished using the 0.2-, 0.25-, and 0.3-mm tool offsets exhibit similar PSD curves measured in the x-direction. Moreover, in the PSD curves measured in the y-direction, neither the PV nor the total PSD significantly

Table 1 Experimental parameters used for tool offset

Polishing pad	LP66
Precession angle (°)	20
Head speed (rpm)	800
Tool offset (mm)	0.20/0.25/0.30
Track spacing (mm/pitch)	0.75
Surface feed (mm/min)	4000

Fig. 5 Surface profiles obtained with tool offsets of (a) 0.20, (b) 0.25, and (c) 0.30 mm



affects the surface profiles because they are virtually identical. Thus, the tool offset does not significantly affect the surface profiles and is only proportional to the MRR. In this stage of the experiment, a 0.3-mm tool offset is used as the experimental parameter to obtain a high-efficiency MRR.

3.2 Head speed

Head speed is a key parameter in bonnet polishing. Lower head speeds cannot provide the ideal material removal profile. Furthermore, extremely high speeds excessively wear the bonnet and causes the polishing machine to vibrate. Thus, the experimental parameters listed in Table 2 are used to examine the relationship between the head speed and the surface profiles.

With increasing head speed, the material removal depth increases [17], and the head speed is proportional to the material

removal depth, as shown in Fig. 7. Furthermore, the number of abrasive particles in the slurry also increases for a particular area per unit of time. At the same feed rate and tool offset, the abrasive particles remove an equal amount of material, according to Eq. (1). Therefore, increasing the head speed and the corresponding rise in the number of abrasive particles leads to an increase in the material removal depth. The increased head speed causes significantly higher surface rippling, as shown in Fig. 8. The corresponding PSD index shown in Fig. 9 demonstrates that higher head speeds lead to MSF errors. With increasing head speeds, the MSF increases. In the x -axis PSD curve, the 0.33-mm^{-1} spatial frequency shows a peak corresponding to a pitch of approximately 3 mm when converted into the transverse axis coordinates of the surface ripple, indicating that a 3-mm pitch regularly appears parallel to the x -axis of the surface ripple, as shown by the blue line. Although higher head speeds generally show higher PSD than the lower head

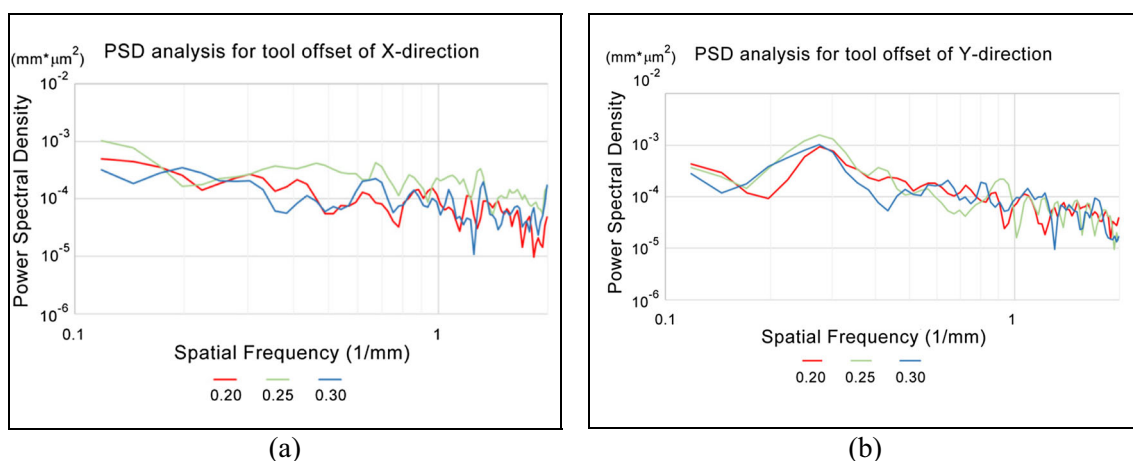


Fig. 6 PSD analysis diagrams obtained for tool offset experiments. **a** x -direction and **b** y -direction

Table 2 Experimental parameters used in head speed experiments

Polishing pad	LP66
Precession angle (°)	20
Head speed (rpm)	300/500/700/900/1000
Tool offset (mm)	0.30
Track spacing (mm/pitch)	0.75
Surface feed (mm/min)	4000

speed curves, at the 0.3-mm^{-1} spatial frequency, all samples have a higher peak value. The surface ripple also indicates that a 3.3-mm pitch regularly appears parallel to the y -axis. The theoretical analysis and experimental results indicate that a lower head speed cannot guarantee excellent material removal capability. A bonnet polishing system for a large aperture is always designed using large components to ensure system strength and rigidity. This experimental result indicates that head speeds higher than 700 rpm produce significant surface ripples, as shown in Fig. 8.

However, using a lower head speed produces a shallow ripple when bonnet polishing. As a lower head speed results in a lower MRR, which consequently leads to lower polishing efficiency, the system cannot obtain an ideal result and subsequently worsens the surface quality of optical glass. Based on these results, a 700-rpm head speed is used in the next series of experiments.

3.3 Track spacing

Track spacing forms a superposition on the polishing path. Thus, the most suitable track spacing parameter should be identified to obtain a good optical surface. From Fig. 9, it is clear that the 0.33-mm^{-1} spatial frequency in the x -direction can be converted into transverse axis coordinates at a pitch of approximately 3 mm, which will regularly generate a surface figure parallel to the x -axis. The surface ripples generated by track spacing form superposition patterns. Because 3 mm is a

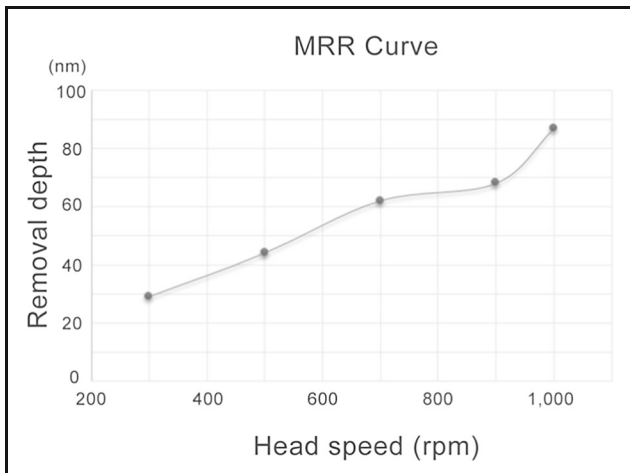


Fig. 7 MRR depth plotted as a function of head speed

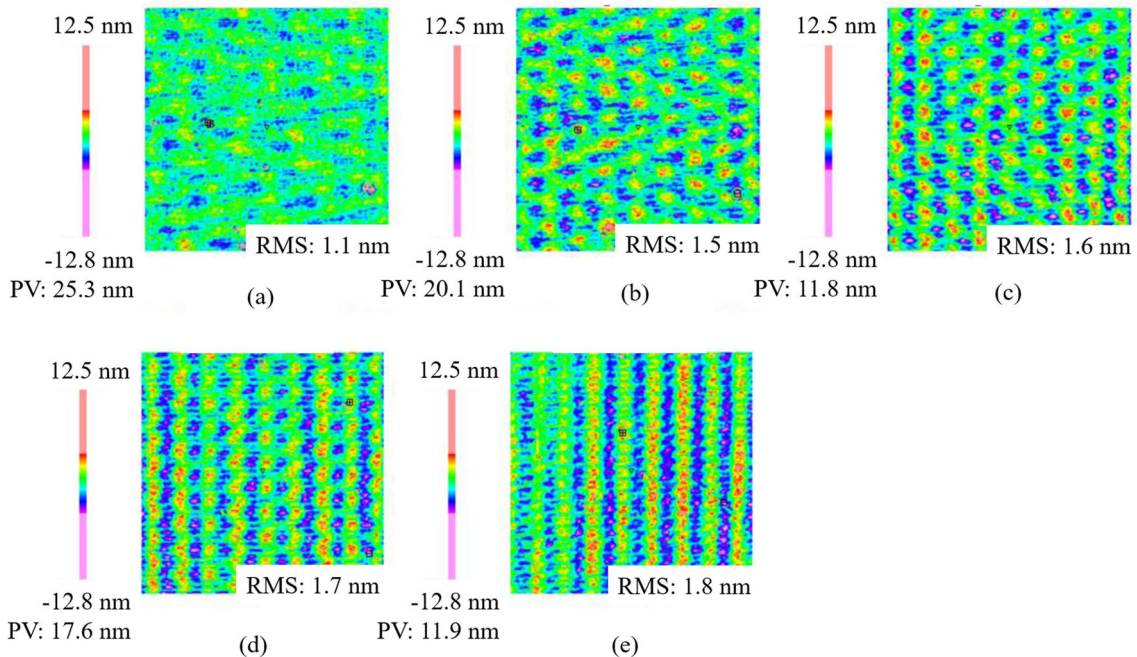


Fig. 8 Surface profiles obtained with the head speeds of (a) 300, (b) 500, (c) 700, (d) 900, and (e) 1000 rpm

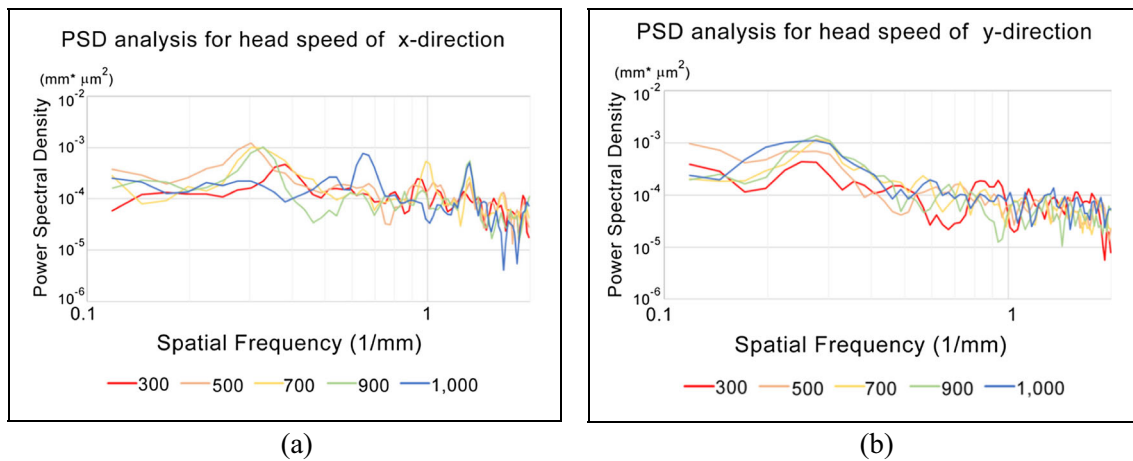


Fig. 9 PSD analysis diagrams for head speed experiments. **a** *x*-direction and **b** *y*-direction

multiple of 0.75, it is reasonable to deduce that the surface figure generated by track spacing shows superposition.

This phenomenon produces serious surface ripples. Considering that 3 mm is not a multiple of the 0.55-mm track spacing, this spacing is also tested to avoid the superposition effect. The head speeds are set as 300, 500, 700, and 900 rpm. The experimental parameters are listed in Table 3. A higher head speed and longer dwell time on the material increase the MRR (Fig. 10). The combination of different head speeds and track spacing produces different surface profiles. The experimental results reveal that the surface profile is significantly improved in the *x*-direction when the 0.55-mm track spacing is used. The surface profile is also uniform in the *y*-direction. However, changing the track spacing parameters does not affect the dwell time or the MRR in the *y*-direction. The 0.55-mm track spacing and 700-rpm head speed produces a fine surface profile, which has a negligible effect on the surface ripple in the *y*-direction, as shown in Fig. 11. Consequently, these spacing and head speed settings are used as the polishing parameter values. The spatial frequency in the *x*-direction PSD curves is observed for different head speeds. For any head speed, a 0.55-mm track spacing induces a significantly improved surface profile compared with a 0.75-mm track spacing, as shown in Fig. 12.

It is worth noting that the surface profile parallel to the *y*-direction is consistent. The 0.75-mm track spacing in the *x*-

direction PSD index has peak values that are suppressed compared with the 0.55-mm track spacing. The 0.75-mm track spacing has a peak value PSD of $10^{-3} \text{ mm} \times \mu\text{m}^2$. In contrast, the 0.55-mm track spacing has a peak value PSD index of $10^{-4} \text{ mm} \times \mu\text{m}^2$ at a 0.33-mm^{-1} spatial frequency. Therefore, the 0.55-mm track spacing can suppress the surface ripple at the 0.33-mm^{-1} spatial frequency.

To avoid varying material removal depths caused by differences in the surface profile, the collocation of equal material removal depths is investigated. The experimental parameters are provided in Table 3. A 0.75-mm track spacing with 500 rpm and a 0.55-mm track spacing with 300 rpm both result in a 48-nm removal depth. A 0.75-mm track spacing with 700 rpm and a 0.55-mm track spacing with 500 rpm both result in a removal depth of 63 nm. Finally, a 0.75-mm track spacing with 900 rpm and a 0.55-mm track spacing with 700 rpm both result in a removal depth of 77 nm. The PSD curves in the *x*-direction grouped by equal material removal depth, as shown in Fig. 13, reveal that using the 0.55-mm

Table 3 Experimental parameters used for track spacing

Polishing pad	LP66
Precession angle (°)	20
Head speed (rpm)	300/500/700/900
Tool offset (mm)	0.30
Track spacing (mm/pitch)	0.55/0.75
Surface feed (mm/min)	4000

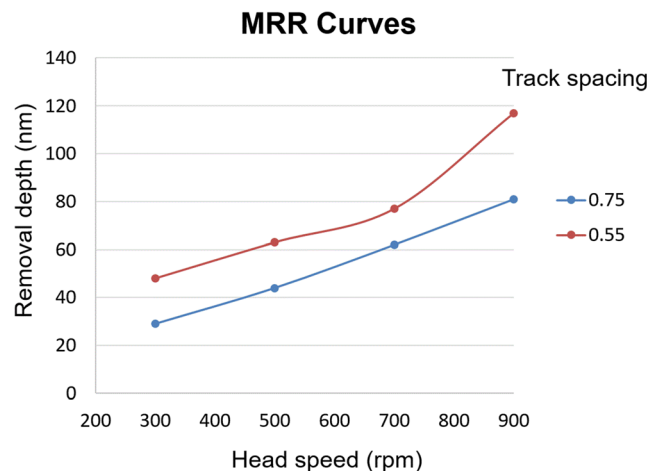


Fig. 10 Removal depth plotted as a function of head speed

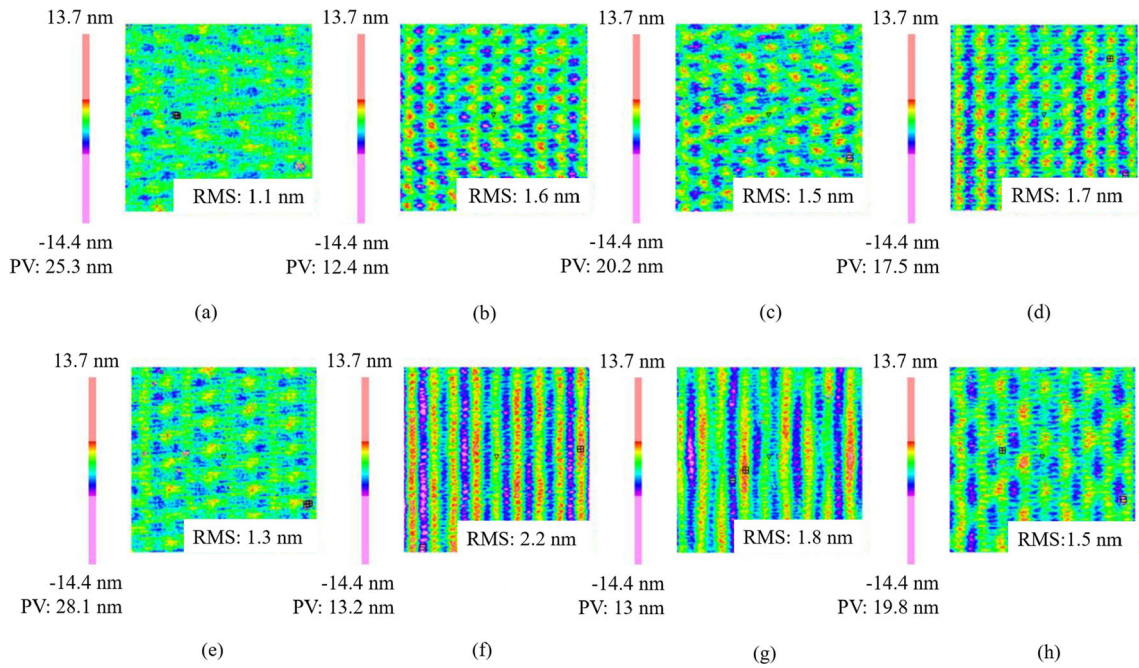


Fig. 11 Surface profiles obtained for track spacing experiments. Track spacing, 0.75 mm: (a) 300, (b) 500, (c) 700, and (d) 900 rpm. Track spacing, 0.55 mm: (e) 300, (f) 500, (g) 700, and (h) 900 rpm

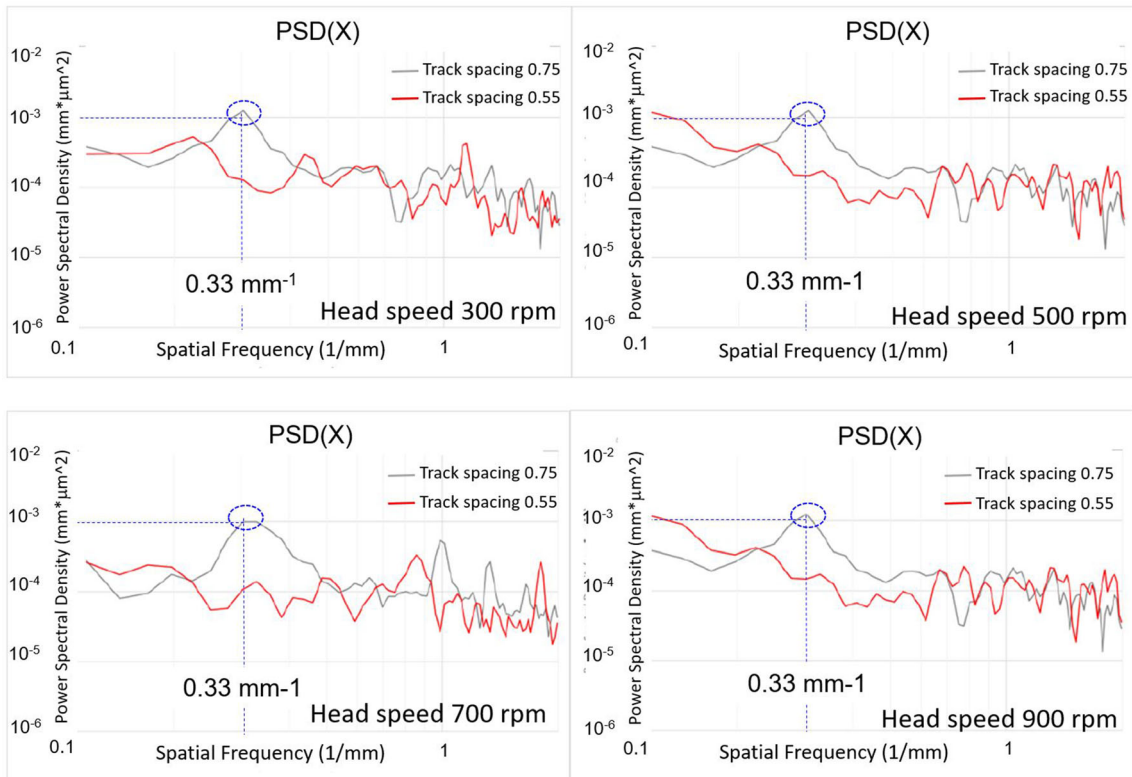
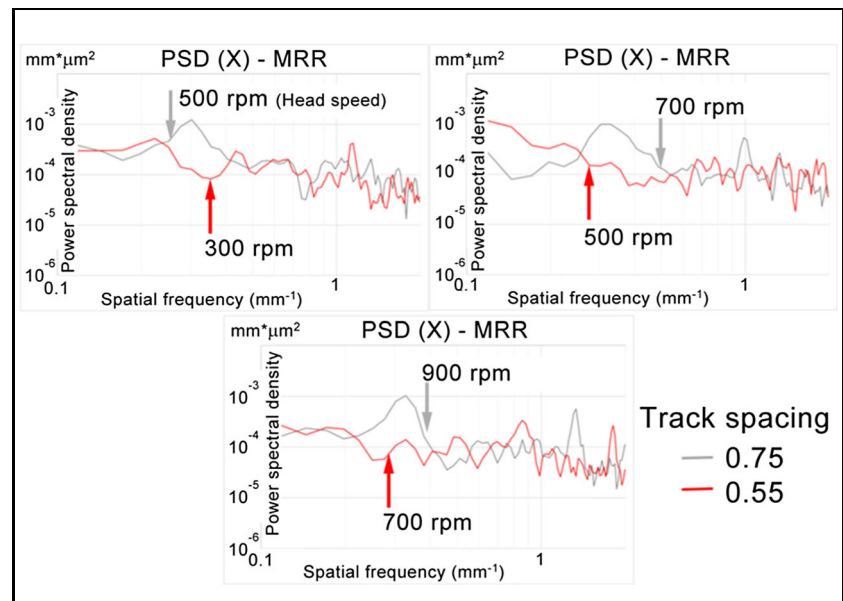


Fig. 12 PSD analysis diagrams for x-direction in track spacing experiments

Fig. 13 PSD analysis for track spacing experiments at the same MRR



track spacing can effectively reduce x -direction surface ripple and further provide fine surface quality. In the follow-up experiment, a 0.55-mm track spacing is used.

3.4 Surface feed rate

The surface feed rate directly affects the dwell time and further affects the surface profile of optical glass during bonnet polishing. A higher feed rate can provide higher surface quality but is limited to the 500–4500 mm/min

range by the feed rate of the machine. Therefore, the feed rate is set in the range that most operators use for bonnet polishing optical lenses. In this surface feed rate experiment, the previous experimental results after optimization are utilized to obtain the appropriate combination of polishing parameters. Consequently, a 700-rpm head speed, 0.3-mm tool offset, and 0.55-mm track spacing are used as the experimental parameters for the surface feed rate, as shown in Table 4. Although a high-quality surface is achieved, it still exhibits superposition in every

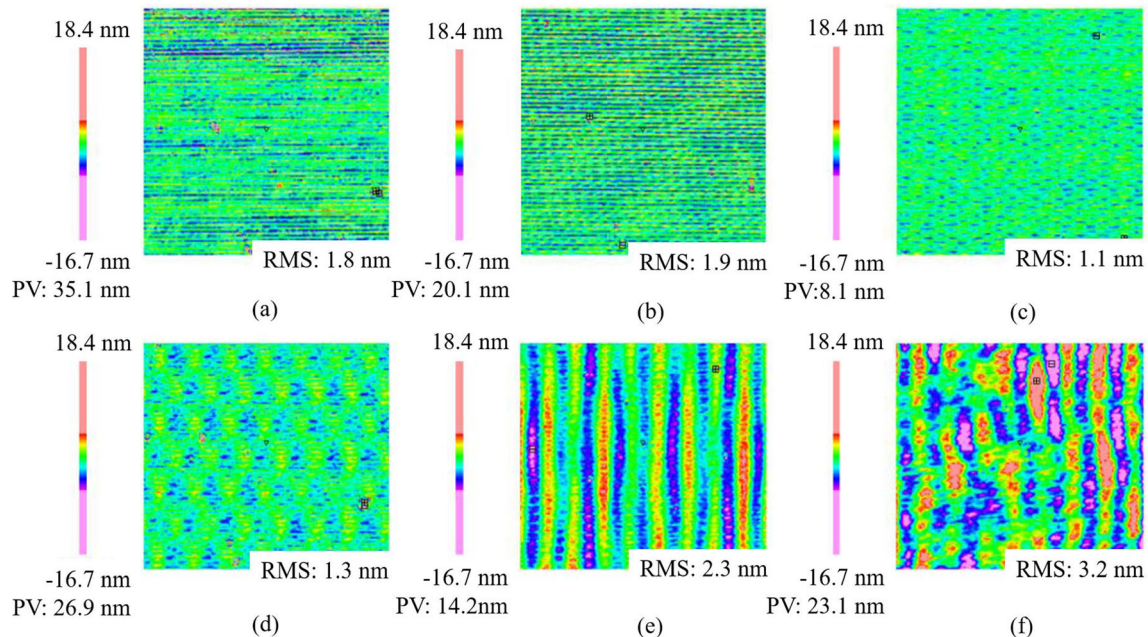


Fig. 14 Surface profiles obtained in surface feed rate experiments. (a) 500, (b) 1000, (c) 2000, (d) 3000, (e) 4000, and (f) 4500 mm/min

Table 4 Experimental parameters for surface feed rate

Polishing pad	LP66
Precession angle (°)	20
Head speed (rpm)	700
Tool offset (mm)	0.30
Track spacing (mm/pitch)	0.55
Surface feed (mm/min)	500/1000/2000/3000/4000/4500

pass. This regular and obvious surface ripple directly affects the image quality of optical lenses because it has a closer track spacing that cannot be removed easily by post-processing. The surface ripple appears parallel to the *x*-direction through superposition from track spacing, as shown in Fig. 14.

Surface ripples at higher surface feed rates are very shallow because they have a shorter dwell time to maintain the removal depth. For surfaces polished using high surface feed rates, the surface ripple originates from factors such as the bonnet pressure, tool offset, and machine vibration. At lower frequencies, a major amplitude vibration appears parallel to the *y*-direction of the surface profile. In contrast to the behavior in the *x*-direction, increasing the surface feed rate improves surface ripples. In addition, the *x*-direction PSD curve for surface feed rate experiments is observed. When the surface feed rate is 1000 rpm or lower, the PSD curve reaches its highest peak value because superposition induces energy concentration, which increases the PSD, as shown in Fig. 15.

In addition, the *y*-direction PSD for the surface feed rate is observed; thus, surface feed rates of higher than 4000 mm/min exhibit poor energy concentration performance. At a spatial frequency of 0.3 mm⁻¹, there is a peak value that is mainly induced by the energy concentration at a specific frequency in machine motion. In

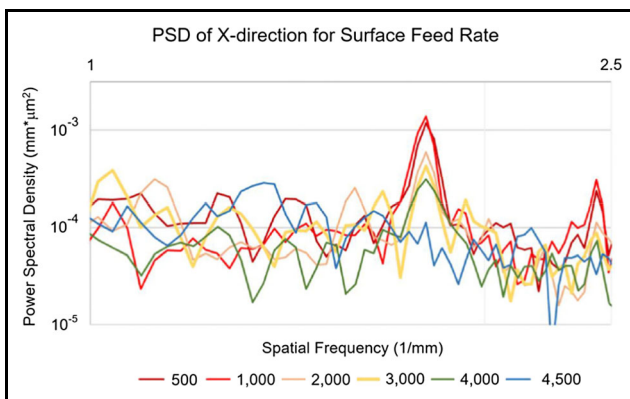


Fig. 15 *x*-direction PSD analysis for surface feed rate experiments

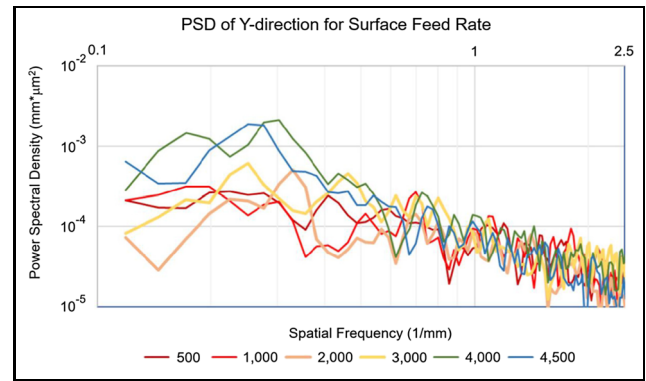


Fig. 16 *y*-direction PSD analysis for surface feed rate experiments

other words, a 3.3-mm surface ripple from the machine vibration appears parallel to the *y*-direction, as shown in Fig. 16.

As this result indicates, a lower surface feed rate shows evident surface polishing marks parallel to the *x*-direction in every pass because of superposition with closer track spacing. Furthermore, a higher surface feed rate suffers from machine vibration caused by the regular vibration frequency, which affects the surface profile. To identify the appropriate surface feed rate, the surface profile is measured with an interferometer for each experiment. The original surface profile is subtracted from the polished surface profile to obtain the actual polishing surface profile, and a Zernike removal filter is used to subtract the first 36 items, including the tilt and original surface profile. Subsequently, the two-direction position and its point data are separately sliced, and the RMS error (RMSE) value is calculated under different surface feed rate parameters. The equation for the RMSE follows:

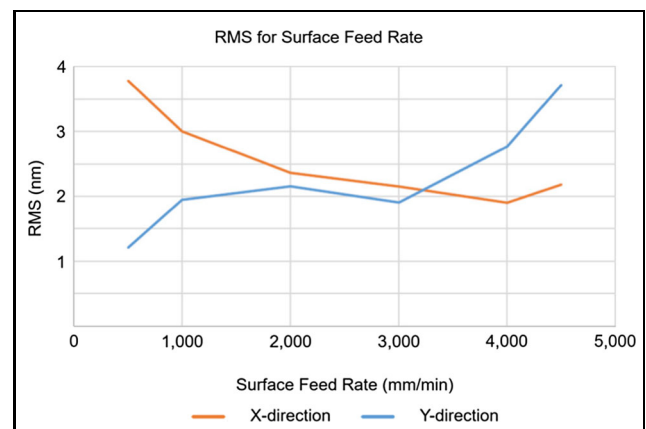


Fig. 17 RMSE analysis of surface feed rate

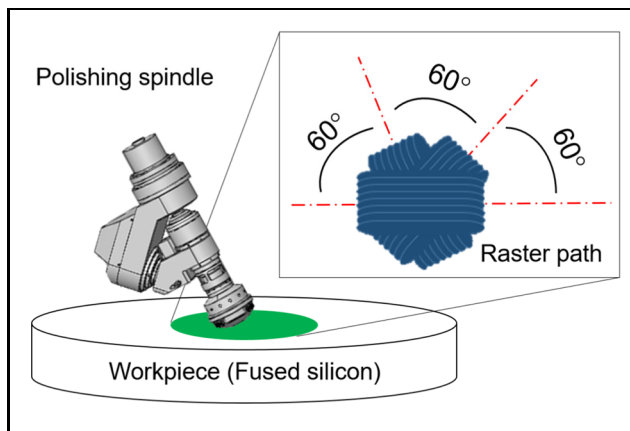


Fig. 18 Path design for equal amounts of material removal

$$RMSE = \sqrt{\frac{\sum_{i=1}^n (Z_{meas,i} - Z_{model,i})^2}{n}} \quad (2)$$

where RMSE, n , Z_{meas} , and Z_{model} represent the root mean square error, sample number, measured value, and model value, respectively. Figure 17 shows that lower surface feed rates increase the RMSE in the x -direction because they yield a surface ripple owing to track spacing superposition; higher surface feed rates increase the RMS in the y -direction because they develop a ripple from machine vibration. Therefore, surface feed rates of less than 1000 mm/min or higher than 4000 mm/min are not recommended. Thus, surface feed rates between 1500 and 3500 mm/min are used to avoid worsening the surface profile in any direction.

3.5 Experiment for equal amounts of material removal

To equally distribute the superposition paths, the polishing passes are divided from 180° into three part, such that the rotation table is placed once every 60° . This process enables repeated multiple distributions of

Table 5 Experimental parameters for equal amounts of material removal

Polishing pad	LP66
Precession angle ($^\circ$)	20
Head speed (rpm)	700
Tool offset (mm)	0.30
Track spacing (mm/pitch)	0.55
Surface feed (mm/min) \times times	$1500 \times 3/2000 \times 4/2500$ $\times 5/3000 \times 6/3500 \times 7$

Experiment of equal amount of material removed

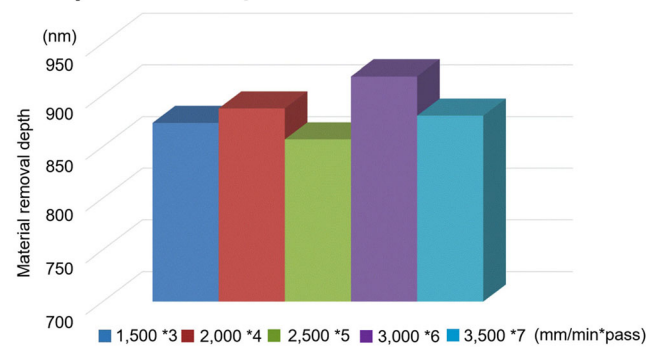


Fig. 19 Comparison for equal amounts of material removal

different feed rates to obtain extremely high-quality optical glass surfaces [18]. The experimental parameters for equal amounts of material removal are listed in Table 5 and Fig. 18. In the experiments with equal amounts of material removal and a surface analysis, the material removal depth is found to range from 850 to 920 nm with an error of approximately 6.6%, as shown in Fig. 19, suggesting that the optimization parameters have good reliability. QED-ASI interferometer is used to analyze the surface profiles of the bonnet-polished optical glasses.

This measurement provides the surface profile data after subtracting the original surface profile from the polished surface profile. The same dwell time is applied to a unit region to ensure removal of an equal amount of material [19]. The surface profiles with an equal amount of material removed are shown in Fig. 20.

The surface profile data and the PSD index of the equal material removal amounts shown in Figs. 20 and 21 indicate that the PV, and RMS values are greatly improved when the feed rate is optimized. As shown in Fig. 20a, a 1500-mm/min feed rate is used to achieve excellent surface quality. The greater uniformity of the colors implies that excellent PV and RMS values of 29.9 nm and 1.6 nm, respectively, are obtained. The PSD analysis additionally indicates that the 1500-mm/min feed rate results in lower PSD values; along with the three times single pass machining, this implies that a weak energy concentration and a smooth surface are obtained. Thus, the PSD index demonstrates that the 1500-mm/min feed rate provides excellent performance compared with the other feed rates, as shown in Fig. 21.

Using the Zernike removal filter and extracting five different positions of the section point data of the optical surface, the RMS deviation is analyzed using Eq. (2). The RMS analysis results are shown in Fig. 22. To evaluate the surface quality of the optical surface performance, the

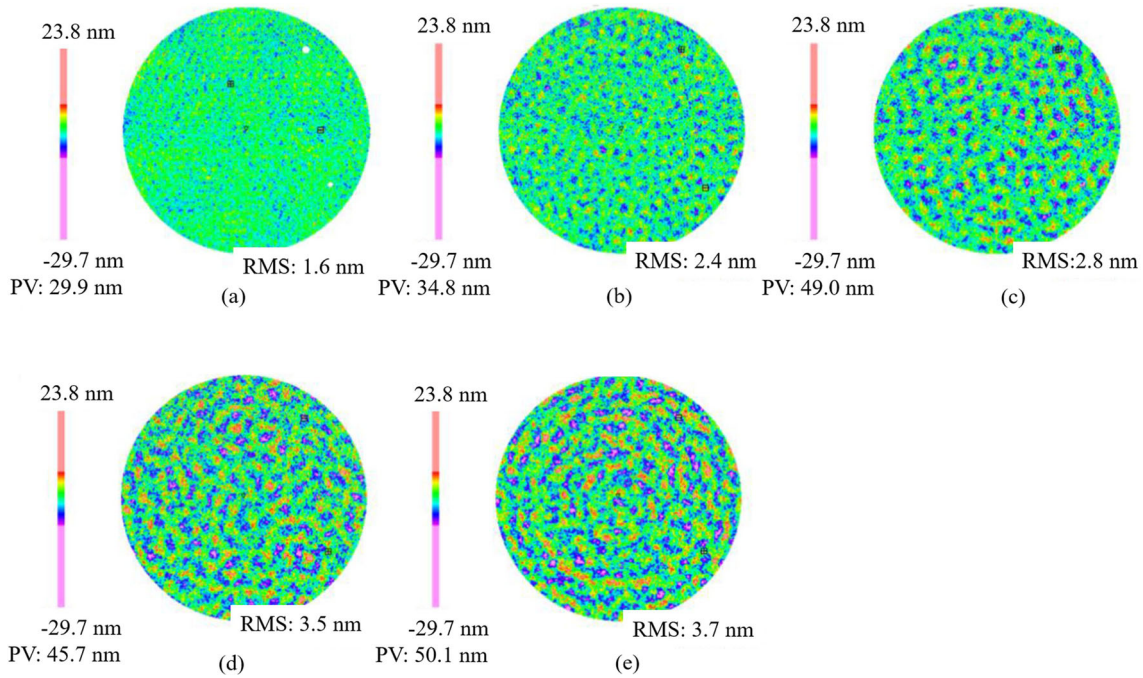


Fig. 20 Surface profile of the samples for equal amounts of material removal. (a) 1500 mm/min × 3, (b) 2000 mm/min × 4, (c) 2500 mm/min × 5, (d) 3000 mm/min × 6, and (e) 3500 mm/min × 7

RMS analysis plot is used. The combination of parameters with the 1500-mm/min feed rate for the polishing head provides a lower RMSE when obtaining smooth surface quality and excellent surface profile accuracy. Based on the experimental analysis and results for equal material removal, the combination of parameters with the 1500-mm/min feed rate as the final optimized combination is recommended in the bonnet polishing process. This method can be applied to remove the sub-surface failure layer and obtain a smooth surface.

4 Experimental verification

To examine the repeatability of optimized parameters, three runs of repeatability experiments were performed on the

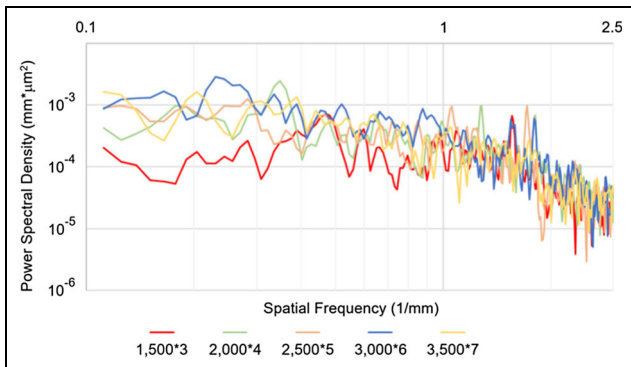


Fig. 21 PSD for equal amounts of material removal

optical glass with diameter 100 mm. As shown in Fig. 23, the results of PV and RMS values in repeatability experiments are similar.

The repeatability statistical results, as listed in Table 6, agree with the outcome mentioned above; it also reveals that a fairly smooth surface texture could be obtained. These results lead to the summary that the optimized parameters can be proved to be reliable in repeated experiments.

In the next stage, to verify the reliability of the optimized parameters, the previous and current experiments both with and without optimized parameters are compared. Based on the

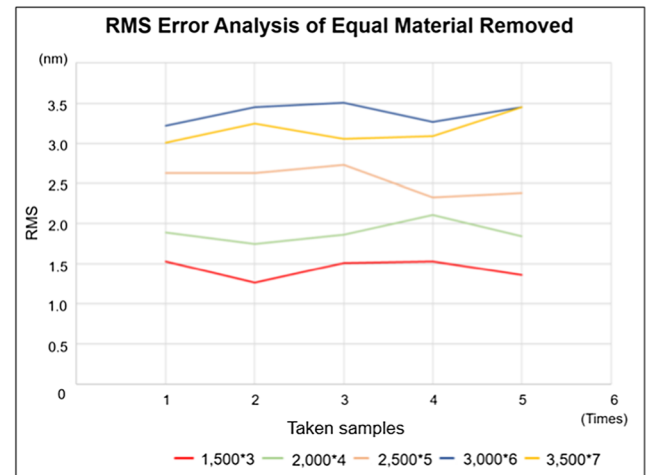


Fig. 22 RMSE analysis for equal amounts of material removed

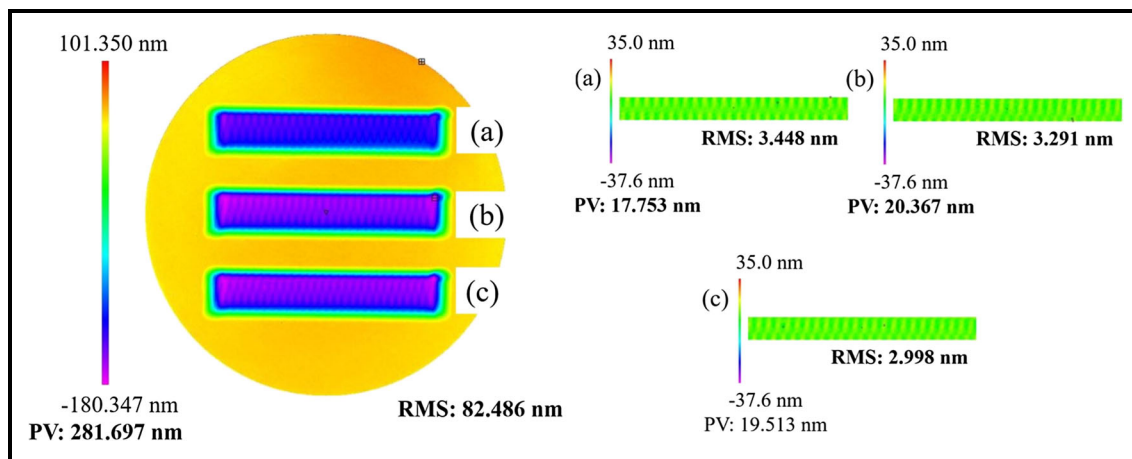


Fig. 23 Surface texture of repeatability test for (a) first, (b) second, and (c) third run

previous experimental analysis and discussion, the optimization parameters are listed in Table 7.

The optimization parameters include the tool offset, head speed, track spacing, and surface feed rate. Other polishing parameters, such as the polishing pad, precession angle, and polish path, are fixed. Therefore, the LP66 polishing pad, a 20° precession angle, and the raster path are adopted as fixed parameters. When referring to the analysis and discussion of the experimental results (Section 3.1), the tool offset is set to 0.3 mm as an optimization parameter, as it can obtain a higher-efficiency MRR compared with the tool offsets of 0.2 mm and 0.3 mm. For the optimization parameter of head speed (Section 3.2), 700 rpm is selected because it provides an excellent PV and PSD curve. Using a lower head speed results in a lower MRR; on the contrary, a head speed above 700 rpm would produce serious surface ripple and degrade the surface quality. The optimization parameter of track spacing was adapted as 0.55 mm (Section 3.3) due to the track spacing of 0.75 mm possesses an obvious noise at the frequency of 0.33/mm and a higher total PSD index and that means worse surface quality. As a result, we used 0.55-mm track spacing as an optimization

parameter. The optimization parameter of the surface feed rate (Section 3.4) is set at 1500 mm/min because a lower surface feed rate would lead to superposition-induced energy concentration. Figure 24 shows the measurement results of the surface texture tests via QED-ASI interferometer. The results show that various types of surface texture can be generated using different polishing parameters. The optimized parameters directly affect the surface texture quality. The surface texture obtained using the optimized parameters in LP66 bonnet polishing is shown in Fig. 24a. This implies that there is less residual surface texture and it approaches the same lane. In contrast, in the previous experiment as shown in Fig. 24b, obvious middle spatial frequency texture is left. In the numerical analysis, the RMS value of surface texture obtained by using optimized parameters is 1.6 nm, whereas RMS value of surface obtained without using the optimized parameters is 18.2 nm. In this verification stage, we considerably reduced the residual error on optical glass and obtained a high-quality surface texture. The evidence can also express that using a strategy of multi-polishing runs with different direction paths can further improve RMS value, for example, from mean value 3.2 nm obtained

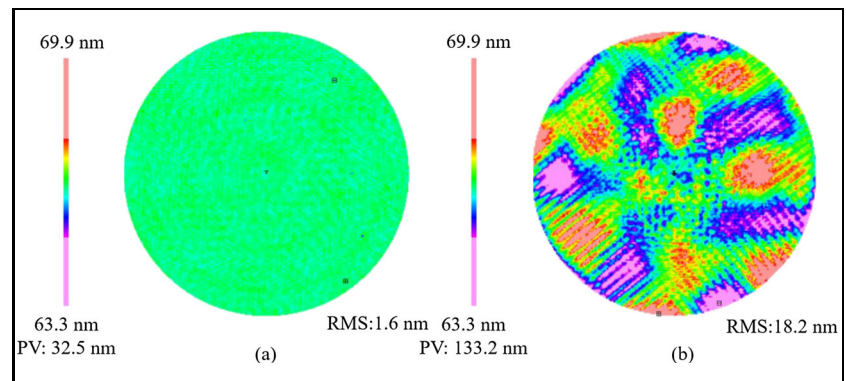
Table 6 Repeatability statistical polishing results with optimized parameters

Test run	Surface texture (unit nm)	
	PV	RMS
First	17.753	3.448
Second	20.367	3.291
Third	19.513	2.998
Mean value	19.211	3.246
S.D.	1.088	0.186

Table 7 Optimization parameters used in verification experiments

Polishing pad	LP66
Precession angle (°)	20
Tool offset (mm)	0.30
Head speed (rpm)	700
Surface feed rate (mm/min)	1500
Track spacing (mm/pitch)	0.55
Polishing path	Raster

Fig. 24 Comparison of surface texture in LP66 bonnet polishing (a) with optimized parameters and (b) without optimized parameters



from repeat test to 1.6 nm obtained by previous study. This is because that when one polishing process is divided into two polishing processes with different direction path, the features left by first polishing run can be crushed into smaller parts by second polishing run. It will make the RMS value become smaller, and that means better surface quality.

5 Conclusions

In this study, theoretical and experimental investigations are conducted to determine optimized parameter combinations for improving the surface texture quality. Bonnet polishing is used to determine the effects of various polishing parameters on the surface texture quality of fused silica obtained using the LP66 bonnet. The main findings are summarized as follows:

1. Although the tool offset affects the MRR, it does not affect the surface texture during bonnet polishing. The large tool offset producing the highest MRR was selected to reduce the polishing time and provide excellent polishing efficiency.
2. When the polishing machine is used to meet the requirements of the large workpiece, the machine vibrations affect the surface texture. Therefore, 700 rpm was selected as the optimized parameter because it demonstrates the best combination of material removal efficiency and excellent surface texture.
3. To avoid the machine vibration caused by the fixed frequency texture of the surface, the track spacing was optimized to 0.55 mm.
4. When the feed rate is less than 1000 mm/min, the reciprocal overlapping of the polishing paths results in significant material removal. Therefore, the feed rate should be in the 1500–3500 mm/min range.

These experimental results demonstrate that the LP66 polishing pad provides high efficiency, high quality, and

excellent performance with the optimal parameters; a smooth surface of optical glass with a 1.6-nm RMS value can be achieved after polishing. Through a series of optimization experiments, irregular surface profiles could be effectively removed, and MSF errors could also be reduced. The repeatability statistical results indicate that the experiment results for PV and RMS are similar and a smooth surface texture can be obtained. These results demonstrate the applicability of LP66 in CNC bonnet polishing for extremely accurate freeform optical components. This process can be used in high-powered laser and UV-lithographic optics applications.

Acknowledgments We appreciate the invaluable expert comments and advice on the manuscript received from Ching-Hsiang Kuo, Zong-Ru Yu, Cheng-Fang Ho, and Hong-Tsu Young.

Funding information The authors declare that there are no financial interests or other potential conflicts of interest involved in the preparation and publication of this manuscript. This study was financially supported by the Ministry of Science and Technology of Taiwan project through technical cooperation and shared technical experience relevant to polishing technology between National Taiwan University and Taiwan Instrument Research Institute, National Applied Research Laboratories.

Compliance with ethical standards

Conflict of interest The authors declare that there are no conflict of interest.

References

1. Yakubov VP, Kamenev AV, Ponomarev SV (2017) Spherical lens-reflector for aerospace communication. Progress in Electromagnetics Research Symposium—(PIERS), St. Petersburg, Russia (May 22–25, 2017), No. 17521109. <https://doi.org/10.1109/PIERS.2017.8262439>
2. Blackmore-Wright S, Eperjesi F (2012) Blue-light filtering intraocular lenses. Eur Ophthalmic Rev 6:104–107. <https://doi.org/10.17925/EOR.2012.06.02.104>
3. Cheung CF, Li HF, Lee WB, To S, Kong LB (2007) An integrated form characterization method for measuring ultra-precision free form surfaces. Int J Mach Tool Manu 47:81–91. <https://doi.org/10.1016/j.ijmactools.2006.02.013>

4. Cheung CF, Kong LB, Ren M, Whitehouse D, To S (2012) Generalized form characterization of ultra-precision freeform surfaces. *CIRP Annals–Manu Tech* 61:527–530. <https://doi.org/10.1016/j.cirp.2012.03.015>
5. Cao ZC, Cheung CF (2014) Theoretical modelling and analysis of the material removal characteristics in fluid jet polishing. *Int J Mech Sci* 89:158–166. <https://doi.org/10.1016/j.ijmecsci.2014.09.008>
6. Walker DD, Beaucamp ATH, Doubrovski V, Dunn C, Evans R, Freeman R, Kelchner J, McCavana G, Morton R, Riley D, Simms J, Yu G, Wei X (2006) Automated optical fabrication: first results from the new “precessions” 1.2 m CNC polishing machine. *Proc SPIE* 6273, *Optomechanical Technologies for Astronomy*, No. 627309. <https://doi.org/10.1117/12.671098>
7. Beaucamp A, Namba Y (2013) Super-smooth finishing of diamond turned hard X-ray molding dies by combined fluid jet and bonnet polishing. *CIRP Annals–Manu Tech* 62:315–318. <https://doi.org/10.1016/j.cirp.2013.03.010>
8. Hoyo JD, Kim DW, Burge JH (2013) Super-smooth optical fabrication controlling high spatial frequency surface irregularity. *Proc SPIE* 8838, *Optical Manufacturing and Testing X*, No. 88380 T. <https://doi.org/10.1117/12.2022924>
9. Wang CJ, Cheung CF, Ho LT, Liu MY, Lee WB (2017) A novel multi-jet polishing process and tool for high-efficiency polishing. *Int J Mach Tool Manu* 115:60–73. <https://doi.org/10.1016/j.ijmactools.2016.12.006>
10. Wang C, Yang W, Wang Z, Yang X, Sun Z, Zhong B, Pan R, Yang P, Guo Y, Xu Q (2014) Highly efficient deterministic polishing using a semirigid bonnet. *Opt Eng* 53:1–9. <https://doi.org/10.1117/1.OE.53.9.095102>
11. Belkhir N, Aliouane T, Bouzid D (2014) Correlation between contact surface and friction during the optical glass polishing. *Appl Surf Sci* 288:208–214. <https://doi.org/10.1016/j.apsusc.2013.10.008>
12. Guo J, Beaucamp A, Ibaraki S (2017) Virtual pivot alignment method and its influence to profile error in bonnet polishing. *Int J Mach Tool Manu* 122:18–31. <https://doi.org/10.1016/j.ijmactools.2017.06.001>
13. Cao Z, Cheung CF, Zhao X (2016) A theoretical and experimental investigation of material removal characteristics and surface generation in bonnet polishing. *Wear* 360–361:137–146. <https://doi.org/10.1016/j.wear.2016.03.025>
14. Pan R, Zhong B, Chen D, Wang Z, Fan J, Zhang C, Wei S (2018) Modification of tool influence function of bonnet polishing based on interfacial friction coefficient. *Int J Mach Tool Manu* 124:43–52. <https://doi.org/10.1016/j.ijmactools.2017.09.003>
15. Zeng S, Blunt L (2014) Experimental investigation and analytical modelling of the effects of process parameters on material removal rate for bonnet polishing of cobalt chrome alloy. *Precis Eng* 38:348–355. <https://doi.org/10.1016/j.precisioneng.2013.11.005>
16. Preston FW (1927) The theory and design of plate glass polishing machines. *J Glass Tech.*11. <https://doi.org/10.1299/kikaic.75.2581>
17. Cao ZC, Cheung CF (2016) Multi-scale modeling and simulation of material removal characteristics in computer-controller bonnet polishing. *Int J Mech Sci* 106:147–156
18. Walker DD, Brooks D, King A, Freeman R, Morton R, McCavana G, Kim SW (2003) The “precessions” tooling for polishing and figuring flat, spherical and aspheric surfaces. *Opt Express*, 11: 958–964. <https://doi.org/10.1364/OE.11.000958>
19. Yang MY, Lee HC (2001) Local material removal mechanism considering curvature effect in the polishing process of the small aspherical lens die. *J Mater Process Technol* 116:298–304. [https://doi.org/10.1016/S0924-0136\(01\)01055-X](https://doi.org/10.1016/S0924-0136(01)01055-X)

Publisher's note Springer Nature remains neutral with regard to jurisdictional claims in published maps and institutional affiliations.